

Mixed Detonation-Deflagration Behavior of Hydrocarbon-based Rotating Detonation Engines

Takuma Sato and Venkat Raman
University of Michigan
Ann Arbor, MI, USA

1 Introduction and Background

Rotating detonation engines (RDEs) provide a promising approach to increasing efficiency in fossil-fuel based energy extraction, by utilizing detonative combustion processes as opposed to the deflagrations that drive conventional propulsion and energy conversion devices. However, this gain is realizable only when the detonation process can be stabilized and the associated pressure gain can be converted into useful work. Prior studies [1–4] have shown that RDE behavior is highly sensitive to the fuel-air injection process, with the strength of the detonation determined by the level of stratification of the fuel-air mixture within the system [2, 5]. Many of these studies have focused mainly on hydrogen-air detonation, where the high detonability of hydrogen ensures more stable detonation process. In practice, RDEs will use hydrocarbon fuels (methane, ethylene or jet fuels), which are considerably less detonable, and may involve phase change as well. As a result, the behavior of hydrocarbon-based RDEs needs to be understood in detail. Since the detonation behavior is highly sensitive to the mixing process, a detailed description of the complex injection process is necessary.

In this study, the focus is on the mixing and detonation processes within a model RDE configuration experimentally studied at Air Force Research Lab (AFRL), which is an annular configuration operating on ethylene fuel. In the simulations below, it is shown that due to the lower detonability of ethylene (compared to hydrogen) and the specifics of the mixing process, a hybrid detonation-deflagration mode persists within the combustor. In particular, a distributed combustion process driven by a weak azimuthal wave (roughly Ma 1.5) is observed. Below, the details of the geometry and simulation procedure are discussed before the results are presented in Sec. 2.

1 Flow Configuration and Simulation Details

The RDE consists of an annular chamber with an outer diameter of 18.44 cm and an inner diameter of 13.87 cm, with the area ratio between the oxidizer inlet and the detonation chamber being 0.059. The simulation domain is based on the experimental study with ethylene-air of Cho et al [6]. The diameter and gap width are larger compared to their prior hydrogen-based RDE studies to accommodate the large detonation cell size of ethylene-air mixtures. Details of the geometry are provided in Fig. 1. The simulation conditions are described in Table 1. The plenum pressure is computed based on the target mass flow rate. The equivalence

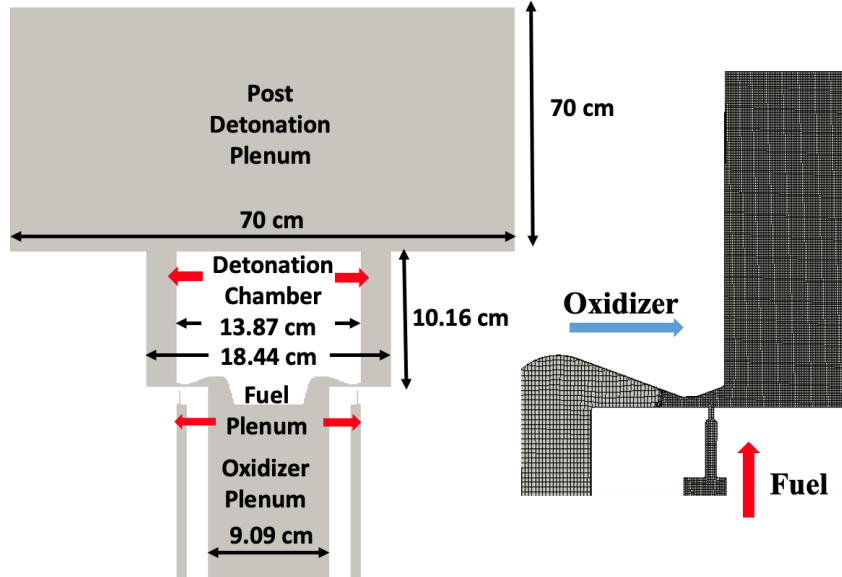


Figure 1: (Left) Details of the geometry and (right) computational mesh near the injector.

ratio is 1.0 for all cases. The variation considered here is related to the inflow temperature, which changes the inflow velocities of the fuel and air jets when the mass flow rates are kept fixed. As will be discussed below, this variation is sufficient to alter the fuel-air stratification within the annular chamber leading to substantial differences in detonation characteristics.

Table 1: Test case description as well as summary of macroscopic results from the simulations.

Composition	Oxidizer plenum P_0 (kPa)	Fuel plenum P_0 (kPa)	Oxidizer plenum T_0 (K)	Fuel plenum T_0 (K)	Air mass flow rate (kg/s)	Back pressure (atm)	$W_{Sim.}$ [m/s]	$W_{Expt.}$ [m/s]
C ₂ H ₄ /Air	441	292	300	300	0.7	1	1070	1020
C ₂ H ₄ /Air	509	292	400	300	0.7	1	1171	–
C ₂ H ₄ /Air	623	292	600	300	0.7	1	–	–

Figure 1 also shows the computational mesh used. An unstructured grid system is used although hexahedral mesh elements dominate the computational domain. The main feature of this combustor is the axial fuel injection port and the radial air port. There are 120 such fuel injection ports around the circumference of the annular chamber, and the full system simulations include the entire set of injection systems and details of the oxidizer feed plenum. A baseline computational grid is generated with a minimum grid spacing of 3×10^{-4} m which results in 30 million cells. Prior study of a similar configuration showed that this resolution is sufficient to adequately capture shock propagation and reaction structure [2, 7].

The computational solver used is the UMDetFOAM [2, 3, 8, 9], which is an in-house solver developed using the open source OpenFOAM package. Detailed chemical kinetics is handled using an interface to CANTERA [10]. In the current study, a reduced mechanism for ethylene-air detonations is used [11]. A MUSCL-based HLLC scheme is used for spatial discretization of the nonlinear convection terms, while

the diffusion terms are handled using the KNP method [12]. The explicit solver is advanced in time using a second-order Runge-Kutta scheme. The solver is highly scalable and can utilize heterogeneous architectures running on hybrid CPU/GPU systems. The validation of the solver and the chemical mechanism is shown in prior studies [2, 7, 13].

2 Results and discussion

Figure 2 shows the pressure field snapshot for the two cases studied here. Two different planes (outer wall and mid-plane) in the radial direction are shown. The 300 K and 400 K cases reveal a visible wave front. The detonation behavior is highly variable across the radial direction, with the shocks showing weaker strength near the mid-plane. More importantly, when the inflow oxidizer temperature is raised to 600 K, the shock structures become significantly weaker, indicating a poor detonation process. Further, even for the 400 K case, it is seen that the detonations are confined to the lower part of the channel, with oblique waves that span the length of the combustor.

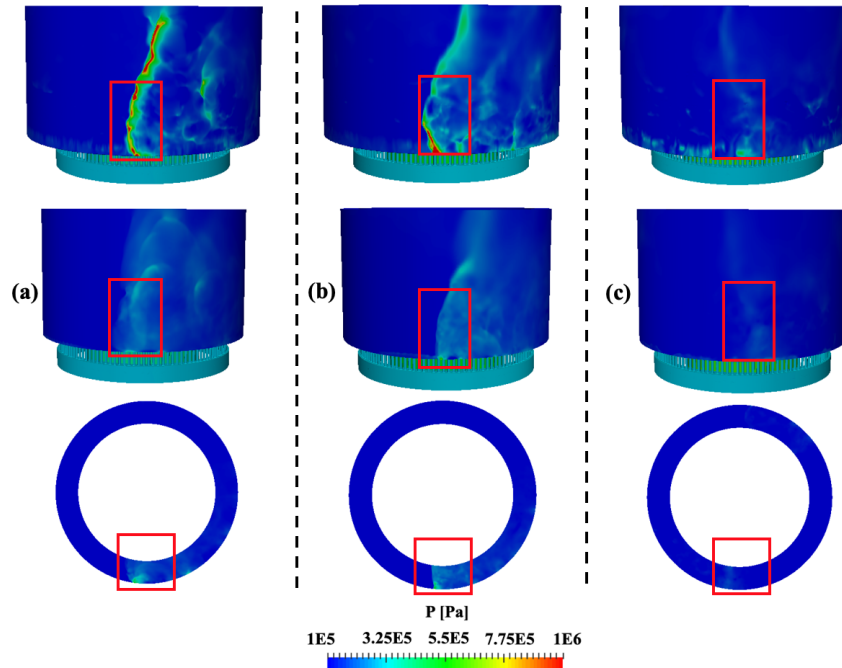


Figure 2: Pressure field of the RDE with ethylene and air chemistry for a) $T_{oxi}^0 = 300$ K, b) $T_{oxi}^0 = 400$ K, and c) $T_{oxi}^0 = 600$ K cases. Top: outer wall. Middle: mid-chamber. Bottom: cutting plane 2 cm from the chamber bottom.

The top row of Fig. 3 shows the equivalence ratio distribution in the cross-section of the combustor near the fuel and air injectors. Although the global equivalence ratio is set to 1.0, there are significant variations in the fuel-air distribution in the near-injector region. In particular, high fuel mass fraction is seen near the bottom of the chamber due to the deflection of the fuel jet by the air crossflow. This flow pattern sets up large scale re-circulation in the chamber, leading to less than ideal mixing in the lower part of the chamber. It is also seen that the 600 K case shows larger fluctuations in equivalence ratio compared to the 300 K and

400 K case. While these are instantaneous images, similar features are observed at multiple time stations. Interestingly, even when the stratification is large close to the outer wall, the detonation structure is strong. This indicates that richer local mixtures (compared to stoichiometric) support detonations while the leaner regions quench the reaction process. If the stratification is too large, this might lead to detonations becoming weaker but is still sustainable.

An analysis of the heat release structure is shown in Fig. 4. In detonative combustion, much of the heat release will happen in the post-shock high-pressure region. In general, these pressures will be in the range of 10-20 atm depending on the fuel mixture. It is seen that for this particular configuration, the peak pressures reach this value. However, heat release itself happens at much lower pressures, comparable to the baseline pressure in the combustor. This feature indicates that the shock wave is detached from the reaction zone, with the strong shock regions located where the equivalence ratio is outside the detonability limits or that the ignition temperature (induction time) is much longer than that provided by a conventional ZND structure. This is further confirmed in the pressure-specific volume plot, also shown in the bottom row of Fig. 3. It is seen that the RDE data lies below the ideal 1D premixed detonation curve (Rankie-Hugoniot line). One way to interpret this data is that the heat release per unit mass is lower than of an ideal mixture. This finding is similar to that reported elsewhere from zero-dimensional analyses [14–16]. Further, it can be seen that the highest pressures observed in the RDE are still lower than the ideal detonation case, indicating that the shocks are weaker.

Finally, Table 1 shows the wave speed in simulation as well as the corresponding experimental data. The experiment data is available only for the 300 K case. The wave velocity for the 600 K could not be obtained because the wave is very unstable with multiple waves appearing and dissipating during one cycle. The wave speed for the 300 K case matches the experiment data within 5 % error.

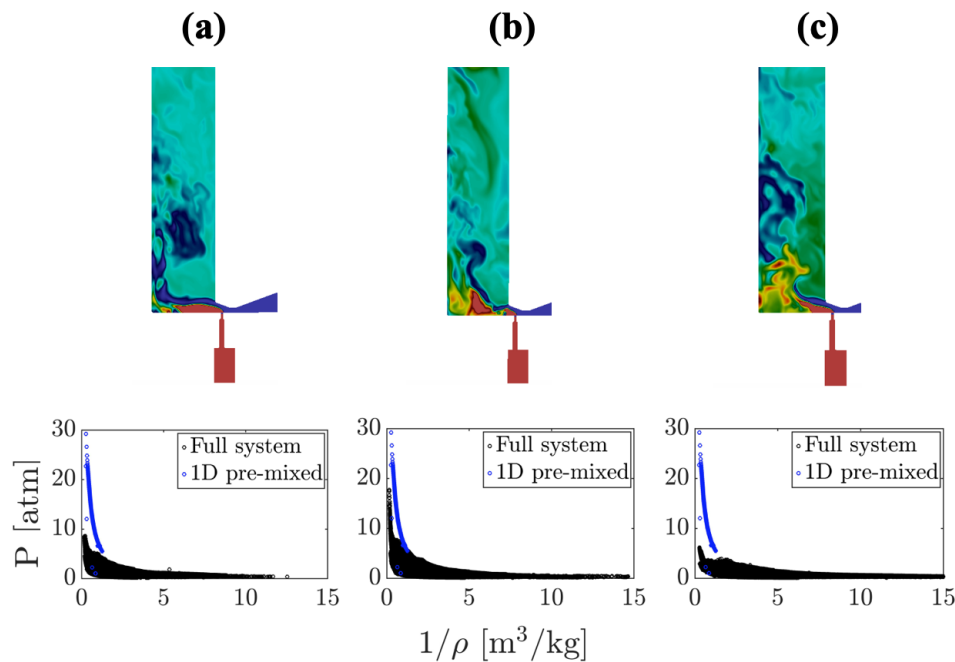


Figure 3: (Top) Equivalence ratio at a cutting plane at the injector location and (bottom) pressure vs. specific volume relation for a) $T_{oxi}^0 = 300$ K, b) $T_{oxi}^0 = 400$ K, and c) $T_{oxi}^0 = 600$ K cases.

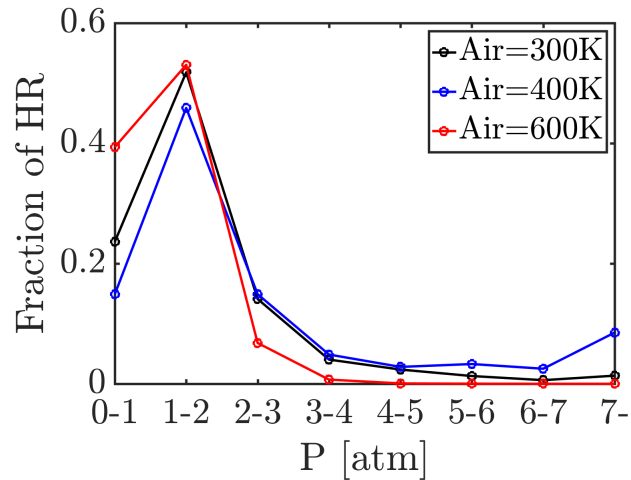


Figure 4: Heat release rate fraction plotted as a function of the local pressure for each case.

3 Conclusions

The ethylene-air RDE simulations show an interesting feature: while there exists a weak shock wave, the combustion process itself is volumetric and distributed, leading to heat release at lower pressures. The pressure profiles show strong variations across the cross-section of the annular chamber. Similarly, the fuel-air mixing is highly non-uniform with large variations close to the outer wall. For the cases studied, variations in inflow velocities of the oxidizer and fuel streams led to large changes in the structure of the detonation processes. In particular, when the flow velocities increased (while keeping the mass flow the same), the stratification was higher. This is primarily due to the lack of small-scale mixing in this design near the injectors, which sets up large-scale recirculation zones in the annular region.

These results clearly show that a mixed detonation-deflagration mode is present in this configuration. The weak shock wave creates minimal compression but induces an azimuthal velocity that creates a trailing mixture of the partially burnt fuel-air mixture. This combustion process is slowly completed as the wave travels around the chamber. As a result, much of the heat-release happens in this trailing mixture rather in the post-shock region. Small changes to the mixing process drastically alter the shock structure. It is expected that any further weakening of the compression process may lead to complete extinction.

We are currently conducting a series of simulations with a) different chemistry mechanisms and b) hydrogen dilution in the fuel in order to assess the effect of these models and parameters on the RDE behavior. More detailed comparisons with experimental data are also being prepared. If selected, these results will be presented at the ICDERS 2019 meeting.

References

- [1] P. A. Cocks, A. T. Holley, and B. A. Rankin, "High fidelity simulations of a non-premixed rotating detonation engine," in *54th AIAA Aerospace Sciences Meeting*, pp. 2016–0125, 2016.
- [2] T. Sato, S. Voelkel, and V. Raman, "Detailed Chemical Kinetics based Simulation of Detonation Containing Flows," in *ASME Turbo Expo*, 2018.

- [3] T. Sato and V. Raman, "Hydrocarbon fuel effects on non-premixed rotating detonation engine performance," in *AIAA Scitech 2019 Forum*, 2019.
- [4] R. Zhou, D. Wu, and J. Wang, "Progress of continuously rotating detonation engines," *Chinese Journal of Aeronautics*, vol. 29, no. 1, pp. 15–29, 2016.
- [5] S. Prakash, R. Fiévet, and V. Raman, "The effect of fuel stratification on the detonation wave structure," in *AIAA Scitech 2019 Forum*, p. 1511, 2019.
- [6] K. Y. Cho, J. R. Codoni, B. A. Rankin, J. Hoke, and F. Schauer, "High-repetition-rate chemiluminescence imaging of a rotating detonation engine," in *54th AIAA aerospace sciences meeting*, p. 1648, 2016.
- [7] T. Sato and V. Raman, "Detonation structure in ethylene/air-based non-premixed rotating detonation engine." Submitted to *Journal of Propulsion and Power*, 2019.
- [8] D. Masselot, T. Sato, V. Stephen, and V. Raman, "Development of Robust Computational Tools for Rotating Detonation Engines," *Mediterranean Combustion Symposium*, Sep. 2017.
- [9] M. Hassanaly, H. Koo, C. F. Lietz, S. T. Chong, and V. Raman, "A minimally-dissipative low-Mach number solver for complex reacting flows in OpenFOAM," *Computer and Fluids*, vol. 162, pp. 11–25, 2018.
- [10] D. Goodwin, N. Malaya, H. Moffat, and R. Speth, "Cantera: An Object Oriented Software Toolkit for Chemical Kinetics, Thermodynamics, and Transport Processes, Version 2.1.1," 2012.
- [11] B. Varatharajan and F. Williams, "Ethylene ignition and detonation chemistry, part 2: Ignition histories and reduced mechanisms," *Journal of Propulsion and Power*, vol. 18, no. 2, pp. 352–362, 2002.
- [12] C. J. Greenshields, H. G. Weller, L. Gasparini, and J. M. Reese, "Implementation of semi-discrete, non-staggered central schemes in a colocated, polyhedral, finite volume framework, for high-speed viscous flows," *International journal for numerical methods in fluids*, vol. 63, no. 1, pp. 1–21, 2010.
- [13] T. Sato and V. Raman, "Analysis of detonation structures with hydrocarbon fuels for rotating detonation engines applications." Submitted to *Journal of Propulsion and Power* (10/24/2018), 2018.
- [14] F. Chacon and M. Gamba, "Study of parasitic combustion in an optically accessible continuous wave rotating detonation engine," in *AIAA Scitech 2019 Forum*, p. 0473, 2019.
- [15] J. R. Burr and K. H. Yu, "Mixing in linear detonation channel with discrete injectors and side relief," in *AIAA Scitech 2019 Forum*, p. 1014, 2019.
- [16] J. Humble, S. V. Sardeshmukh, and S. D. Heister, "Reduced order modeling of rotational detonation engines," in *AIAA Scitech 2019 Forum*, p. 0201, 2019.